Physical implications of the extrapolation and statistical bootstrap of nucleon structure function ratios $\frac{F_2^n}{F_2^p}$ for mirror nuclei ³He and ³H

Hannah Valenty, ¹ Jennifer Rittenhouse West ⁰, ² Fatiha Benmokhtar ⁰, ¹ Douglas W. Higinbotham ⁰ Asia Parker, and Erin Seroka⁴

> ¹Department of Physics Duquesne University, Pittsburgh, Pennsylvania 15282, USA ²Lawrence Berkeley National Laboratory, Berkeley, California 94720, USA ³Thomas Jefferson National Accelerator Facility, Newport News, Virginia 23606, USA ⁴Department of Physics, The George Washington University, Washington, DC 20052, USA

(Received 24 November 2022; accepted 16 May 2023; published 13 June 2023)

A nuclear physics example of statistical bootstrap is used on the MARATHON nucleon structure function ratio data in the quark momentum fraction regions $x_B \to 0$ and $x_B \to 1$. The extrapolated F_2 ratio as quark momentum fraction $x_B \to 1$ is $\frac{F_2^n}{F_2^n} \to 0.4 \pm 0.05$ and this value is compared to theoretical predictions. The extrapolated ratio when $x_B \to 0$ favors the simple model of isospin symmetry with the complete dominance of sea quarks at low momentum fraction. At high- x_B , the proton quark distribution function ratio d/u is derived from the F ratio and found to be $d/u \rightarrow 1/6$. Our extrapolated values for both the $\frac{1}{2}$ ratio and the d/u parton distribution function ratio are within uncertainties of perturbative QCD values from quark counting, helicity conservation arguments, and a Dyson-Schwinger equation with a contact interaction model. In addition, it is possible to match the statistical bootstrap value to theoretical predictions by allowing two compatible models to act simultaneously in the nucleon wave function. One such example is nucleon wave functions composed of a linear combination of a quark-diquark state and a three-valence quark correlated state with coefficients that combine to give the extrapolated F_2 ratio at $x_B = 1$.

DOI: 10.1103/PhysRevC.107.065203

I. INTRODUCTION

The ratio of the deep inelastic structure functions F_2^n/F_2^p provides fundamental information about the quark distributions of nucleons [1,2]. In particular, in the limit of the Bjorken scaling variable x_B [3] going to unity, this ratio provides a powerful tool for discriminating between different partonic models. Due to the lack of free neutron targets, it is very challenging to determine the ratio from scattering protons and neutrons; but the use of mirror nuclei, ³H and ³He, and the exploitation of isospin symmetry allow for an accurate determination of this ratio.

The MARATHON experiment at Jefferson Lab has recently published their measured ratios of nucleon structure functions F_2^n/F_2^P with deep inelastic scattering of electrons off of ³H and ³He nuclei [4–11]. Their results cover the quark momentum fraction range $0.19 < x_B < 0.83$ and significantly improve on previous measurements [1,12,13]. The high and low (Fig. 1) Bjorken-x regions were not covered and yet are necessary, especially in the $x_B \rightarrow 1$ regime, in order to distinguish between theoretical predictions for quark and parton behavior at large momentum fraction. The theory predictions differ in their interpretation of the components of the nucleon wave function and how they act in the high- x_B

regime. An example prediction is the scalar diquark model which requires that at $x_B = 1$ only the scalar [ud] diquark plus valence quark component of the nucleon wave function contributes, yielding a structure function ratio of $\frac{1}{4}$. Another example is the SU(6) flavor model in which all vector diquarks (spin-1 and isospin-1 combinations) plus valence quark contribute to give a ratio of $\frac{2}{3}$. Table I presents an inexhaustive list of theoretical predictions, while theory reviews from 1996 [14] and 2010 [15] give comprehensive details and references.

Previous global analyses of parton distibution functions (PDFs) at next-to-next-to-leading order (NNLO) by the CTEQ-TEA (Coordinated Theoretical/Experimental Project on QCD Phenomenology and Tests of the Standard Model) Collaboration give a wide spread of d/u parton distribution function (PDF) ratios [16,17], where PDFs are contained within structure functions. The extrapolation carried out in this work in the high-x region finds d/u values differ-ing from recent fits using the statistical Schlessinger point method, shown in Table II. Our value with uncertainties is within range of three of the theoretical models in Ta-ble I. However, it is possible that more than one theoretical model acts simultaneously in the high-x_B region; for example, a quark-diquark configuration in the nucleon in linear combination with a three-valence quark state can fit our extrapolated value. We discuss this possibility in the next section.

^{*}benmokhtarf@duq.edu

TABLE I. F_2^n/F_2^p model predictions as $x \to 1$. An asterisk indicates that the reference gave a value for the valence quark ratio d/u, from which the F_2 is derived using the isospin symmetry assumptions $u^p = d^n = u$ and $d^p = u^n = d$ and assuming the sea-quark contribution is negligible.

Model	F ₂ ratio prediction	Reference
Scalar diquark $q[ud]$	1/4	[18,19]
Quark model/Isgur	1/4	[20]
Holographic LFQCD	0.282	[21,22]
DSE with qq correlations	0.33	[23] ²
DSE-II contact interaction	0.41	[24,25]
pQCD helicity conservation	3/7	[26]
Quark counting rules	3/7	[27]
Three-quark correlations with CJ12MID	.0.51	[28]
DSE-I dressed quark masses	0.49	[24]
SU(6) Flavor	2/3	[29]
Three-quark correlations with MMHT2014	>0.68	[28] ²

We begin with a theory overview and analysis in the following section and then describe the extrapolation method in detail (Sec. III) before concluding.

II. STRUCTURE FUNCTION THEORY

We start with a review of relevant structure function definitions. The internal structure of nucleons is encoded in the form of structure functions $F_2(x_B, Q^2)$ describing quark and antiquark behavior in terms of parton momentum distribution functions weighted by the square of their electric charge.

Structure functions are components of the deep-inelastic-scattering differential cross section for charged lepton scattering, e.g., $eN \rightarrow eX$,

$$\frac{d^2\sigma}{dt\ du} = \frac{4\pi\alpha^2}{t^2} \frac{1}{2} \frac{1}{s^2(s+u)} [2xF_1(s+u)^2 - 2usF_2], \quad (1)$$

given in terms of the Mandelstam variables for the four-momenta of the incoming lepton p_1 , target p_2 , outgoing lepton p_3 , and hadronized debris p_4 ; $s = (p_1 + p_2)^2$, $t = (p_1 - p_3)^2$; and $u = (p_1 - p_4)^2$. The nucleon structure function F is defined (up to leading order in the strong force coupling α_S) as

$$F_2(x_B) = 2x_B F_1(x_B) = \bigvee_i Q_i^2 x [q_i(x_B) + \overline{q}_i(x_B)], \quad (2)$$

TABLE II. F_2^n/F_2^p fits as $x \to 1$. An asterisk indicates that the reference gave a value for the valence quark ratio d/u, from which the F_2 is derived using the isospin symmetry assumptions $u^p = d^n = u$ and $d^p = u^n = d$ and negligible sea-quark contributions.

Method	F_2 ratio	Reference
Schlessinger point method	≈0.45	[30]
CTEQ	Unconstrained	[16,17]
JAM	≈ 0.4 but x . 0.8	[31]

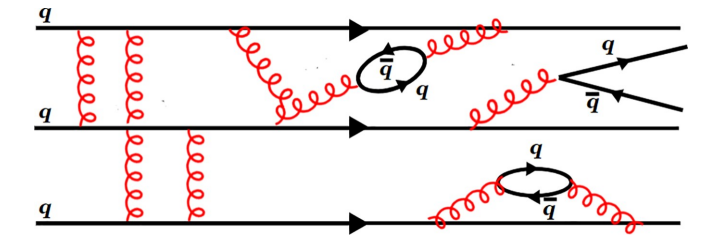


FIG. 1. Example of low-x gluon splitting in a five-quark Fock state of a nucleon. This figure was adapted from Ref. [38].

where the sum is over quark flavors, Q_i^2 is the charge on the *i*th flavor of quark, $q_i(x_B)$ are the quark momentum distribution functions, and Bjorken-*x* is the fraction of nucleon momentum carried by the struck quark. Bjorken-*x* is given in terms of experimental variables

$$x_B = \frac{Q^2}{2M_{\rm T} \mathbf{v}'} \tag{3}$$

where v is the energy lost by the lepton, $E - E^0$, M_T is typically the mass of the struck nucleon in the target, and Q^2 is minus the square of the four-momenta transfer (the vir-tual photon four-momenta squared) $Q^2 \equiv -q^2 = 2EE^0(1 - \cos\vartheta)$, where ϑ is the lepton scattering angle. The subscript B is dropped for notational simplicity from here on out.

The ratios of neutron to proton structure functions F_2^n/F_2^p as measured by the MARATHON experiment and in the regions extrapolated by the statistical bootstrap method on MARATHON data are shown in Figs. 2 and 3, respectively. The model curves in the MARATHON plot are from Kulagin and Petti [32,33], Segarra *et al.* [34], and Accardi *et al.* [35,36]. In brief, these are a phenomenological study, a nucleon universal modification function plus deep-inelastic scattering fit, and a global PDF analysis, respectively. Physical implications and simplifying assumptions of the low and high Bjorken-x behavior are discussed next.

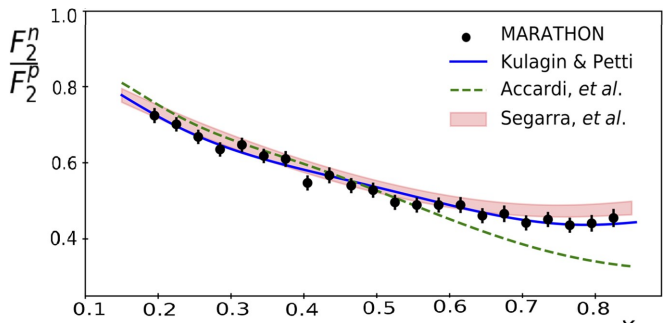


FIG. 2. Deep inelastic scattering F^n/F^p ratios vs x_B from MARATHON [4] compared to theoretical predictions. Error bars include overall systematic uncertainties. Theory curves of Kulagin and Petti [32,33], Segarra *et al.* [34], and Accardi *et al.* [35,36] are discussed briefly in the text. All curves correspond to MARATHON kinematics. This figure is from Kutz [8].

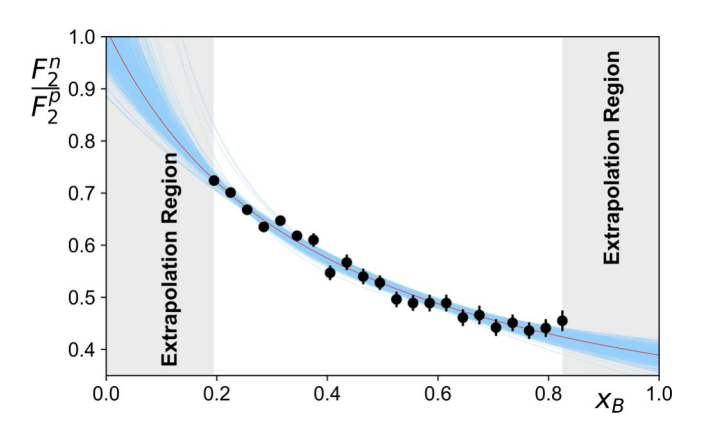


FIG. 3. Fit of the MARATHON data making use of a standard extrapolating function with the uncertainty band determined from statistical bootstrapping. The blue error band is the result of the accumulation of 1000 such fits. The result at $x_B = 1$ indicates a ratio of 0.4 ± 0.05 .

A. Isospin symmetry analysis of extrapolated behavior of F_2^n/F_2^p : $x \to 0$ region

In the low-x region, the process of gluon bremsstrahlung followed by gluon splitting to quark-antiquark pairs dominates the nucleon structure function due to a $\frac{dk}{k}$ probability for gluon splitting (Fig. 1) [37]. The structure function in this region,

$$F_2(x) = \sum_{i}^{X} Q^2 x_i [q_i(x) + \bar{q}_i(x)], \tag{4}$$

contains contributions from the light quark $q\overline{q}$ pairs, $u\overline{u}$, dd, and $s\overline{s}$. Gluon splitting to the heavy mass quarks c, b, and t is neglected as these are highly virtual processes and contribute negligibly to the scattering amplitude.

The structure functions are therefore written as

$$\frac{1}{x}F_{2}^{p}(x) = \frac{4}{9}u^{p}(x) + \frac{1}{9}d^{p}(x) + \frac{4f}{9}u_{s}^{p}(x) + \overline{u}_{s}^{p}(x)^{*} + \frac{1f}{9}d_{s}^{p}(x) + \overline{d}_{s}^{p}(x)^{*} + \frac{1f}{9}s_{s}^{p}(x) + \overline{s}_{s}^{p}(x)^{*}$$
(5)

and

$$\frac{1}{x}F_2^n(x) = \frac{4}{9}u^n(x) + \frac{1}{9}d^n(x) + \frac{4f}{9}u_s^n(x) + \overline{u}_s^n(x) + \frac{1}{9}fd_s^n(x) + \overline{d}_s^n(x) + \frac{1}{9}fs_s^n(x) + \overline{s}_s^n(x), \quad (6)$$

with subscript s denoting sea-quark distributions.

The following assumptions are now made for the quark momentum distribution functions. Strong isospin symmetry assumes u and d form an $SU(2)_{iso}$ doublet (as do p and n) which implies the relations [38]

$$u^{p} = d^{n} \equiv u,$$

$$d^{p} = u^{n} \equiv d,$$

$$s^{p} = s^{n} \equiv s.$$
 (7)

The rest of the analysis is therefore given in terms of the proton's parton distribution functions, the same approximations as used in MARATHON [4].

The structure functions can be rewritten as

$$\frac{1}{x}F_2^p = \frac{4}{9}u + \frac{1}{9}d + \text{ sea terms,}$$

$$\frac{1}{x}F_2^n = \frac{4}{9}d + \frac{1}{9}u + \text{ sea terms.}$$
(8)

For simplicity, assume that the sea-quark distributions are the same as those in Ref. [38],

$$u_s(x) = \overline{u}_s(x) = d_s = \overline{d}_s = s_s = \overline{s}_s \equiv K.$$
 (9)

This assumption does not affect the results.

Then we have

$$\frac{1}{x}F_2^n = \frac{1}{9}(u+4d) + \frac{12}{9}K,$$

$$\frac{1}{x}F_2^p = \frac{1}{9}(d+4u) + \frac{12}{9}K.$$
(10)

When sea-quark momentum distribution functions dominate the structure functions, $K \grave{A} u$ and d, we find

$$\frac{F_2^n}{F_2^p}(x) \to 1 \text{ for } x \to 0. \tag{11}$$

This conclusion agrees with the extrapolated value shown in Fig. 3. Note that it does not depend on the assumption of equal sea-quark distribution functions. It requires only that the *sum* of sea-quark distribution functions be the same for the proton and the neutron, which is essentially a sea-quark version of the isospin symmetry assumptions of Eq. (7).

B. Isospin symmetry analysis of extrapolated behavior of F_2^n/F_2^p : $x \to 1$ region

In the high-x region, for $x \to 1$, the extrapolated ratio $F_2^n/F_2^p \to 0.4 \pm 0.05$. The sea-quark distribution functions become negligible in this region of Bjorken-x and the structure functions are given by

$$\frac{1}{x}F_2^n = \frac{1}{9}(u+4d),$$

$$\frac{1}{x}F_2^p = \frac{1}{9}(d+4u),$$
(12)

where the symmetries of Eq. (7) are again assumed.

For this analysis, we set the ratio equal to the extrapolated value of 0.4 and solve for the ratio of quark distribution functions which may then be compared to data. The result is

$$\frac{F_2^n}{F_2^p} = \frac{\frac{1}{9}(u+4d)}{\frac{1}{6}(d+4u)} = 0.4 \Rightarrow \frac{d}{u} = \frac{1}{6}.$$
 (13)

This value is close to the lower limit of recent work [30],

$$\frac{d^{-1}}{u} = 0.230(57), \tag{14}$$

and is due only to the isospin symmetry arguments of Eq. (7) and the vanishing of sea-quark distributions at high-x. Earlier theoretical work argued that a scalar [ud] diquark forms within the nucleon in the $x_B \rightarrow 1$ limit as a way to lower the energy of the system [19] (Table I). In this version of the scalar diquark model, the highest probability state with a single quark containing all of the nucleon momentum must

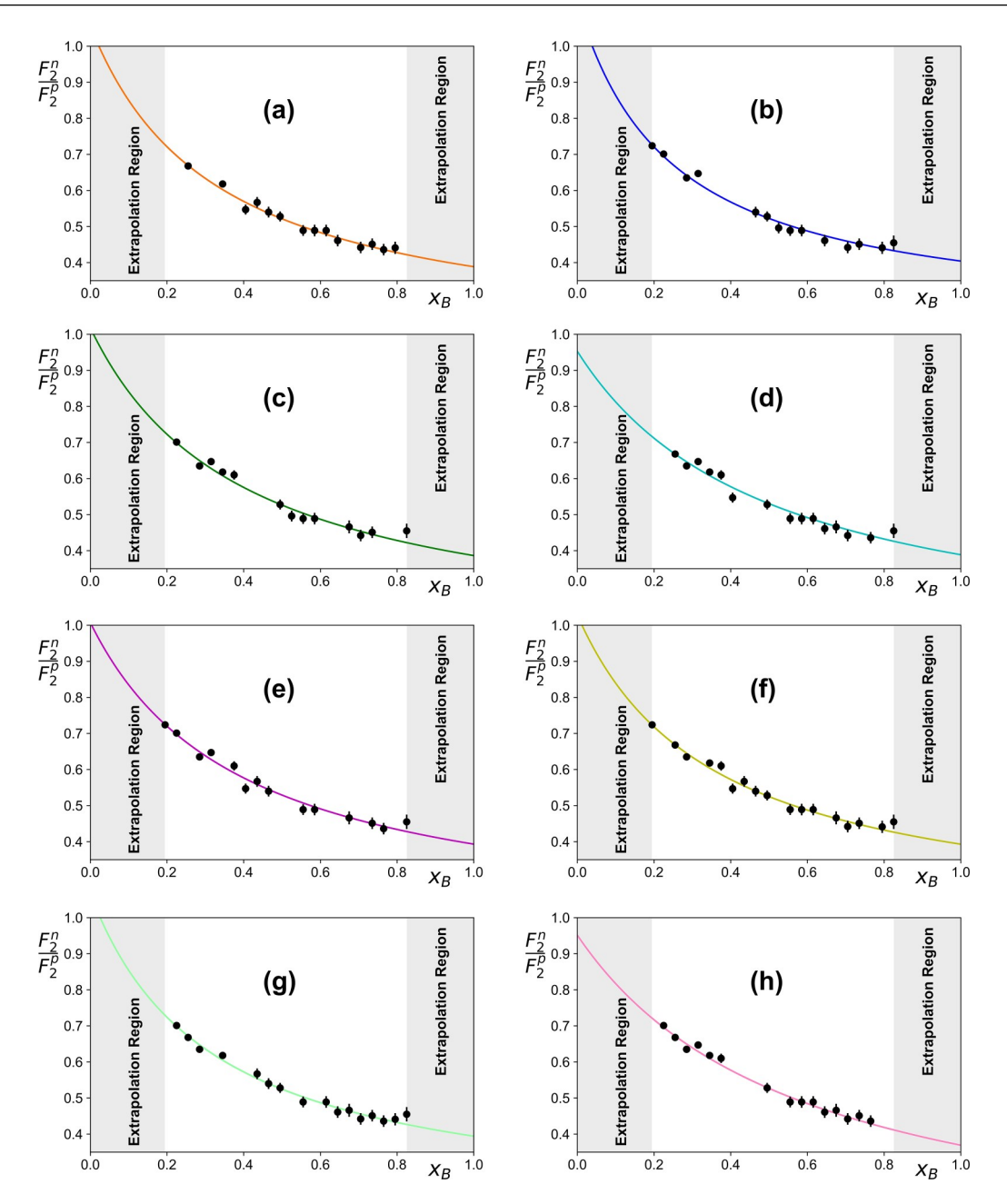


FIG. 4. An eight-panel display of sample plots from the $\approx 10^3$ statistical bootstraps that were performed. The method of uncertainty determination makes use of sampling with replacement and does not require that the data be normally distributed.

minimize the energy of the remaining constituents. Therefore, as $x \to 1$, the lowest-energy proton state is that which has the u quark carrying all the longitudinal momentum with the remaining valence quarks forming the spin-0 isospin-0 [ud] diquark [39] with an estimated binding energy of nearly 150 MeV [40]. Similarly for the neutron with momentum distribution functions swapped, $u \leftrightarrow d$, which gives d/u = 0 in the limit of $x \to 1$. The structure function ratio in this case is given by

$$\lim_{x \to 1} \frac{F_2^n(x)}{F_2^p(x)} = 0.25. \tag{15}$$

Our analysis finds the limiting behavior

$$\lim_{x \to 1} \frac{F_2^n(x)}{F_2^p(x)} = 0.4 \pm 0.05,\tag{16}$$

which disfavors this value. We most closely match the perturbative QCD (pQCD) values using helicity conservation, hard gluon exchange [26], and quark counting rules [27]. The latter two models give the same ratio limit,

$$\lim_{x \to 1} \frac{F_2^n(x)}{F_2^p(x)} = 3/7 \approx 0.43,\tag{17}$$

and these are within the bootstrap uncertainties as shown by the blue band of Fig. 3. There is another physical implication, however, because while some models are incompatible with each other, it is possible that two compatible models could act over the same physical region to give the extrapolated value. One such example is the scalar diquark model with $F_2^n/F_2^P \rightarrow 0.25$ [19] together with the three-quark correlation plus MMHT2014NNLO with $F_2^n/F_2^P > 0.68$ (or CJ12MID with ratio .0.51) from Ref. [28], with different weights given to scalar diquark vs three-quark correlation contributions in order to yield a final ratio of 0.4. The nuclear wave function for A = 3 nuclei has been proposed as a linear combination of nucleons in quark-diquark and three-valence quark configurations, with a range of predictions for short-range correlations [40] which matches the data [41]. We now move on to describing the extrapolation method.

III. STATISTICAL BOOTSTRAP METHOD

Bootstrapping is a technique that allows an estimation of the sampling distribution of almost any statistical distribution using the method of sampling data with replacement. It is any test or metric that falls under the broader class of resampling methods. Bootstrapping assigns measures of accuracy such as variance, confidence interval, and prediction errors to sample estimates [42].

In the case of the MARATHON experiment, a rational function R_f of the form of

$$R_f = n_0 \frac{1 + x n_1}{1 + x m_1} \tag{18}$$

was used to fit the 22 data points corresponding to x_B values between 0.195 and 0.825. n_0 , n_1 , and m_1 are the three fit parameters of this function. The fit was then extrapolated to lower and higher limits of x_B to cover the full range from 0 to 1.

One fit line is created by randomly selecting a set of 22 points from the 22 existing data values allowing one, two, or three substitutions of any of the data points with a randomly chosen value from the same data set. A total of 1000 fits were performed using this method and then plotted to determine the error band. The fits were then extrapolated to lower and higher values of x_B to cover the full range from $x_B \rightarrow 0$ to $x_B \rightarrow 1$.

Panels of selected fits using this statistical bootstrap method are presented in Fig. 4. The blue error band shown in Fig. 3 is the result of the accumulation of 1000 such fits.

IV. CONCLUSION

We have used a statistical bootstrap of the MARATHON deep inelastic scattering data to extrapolate the high and low quark momentum fraction regimes of the $F^n \not/F^P$ ratio. As x_B \rightarrow 1, the ratio F^n/\bar{E}^P approaches 0.4 ± 0.05, which, under the usual isospin symmetry arguments for valence quark par-ton distribution functions of $u^p = d^n = u$ and $d^p = u^n = d$, corresponds to a ratio of $d/u \rightarrow 1/6$. Our extrapolation favors the perturbative QCD helicity conservation, quark counting rules, and DSE with contact interactions models. The scalar diquark model value of the $x_B \rightarrow 1$ limit $F_2^n/F_2^P = 1/4$ is disfavored as are all other models from Table I. We note that, while many models are incompatible with each other, it is possible that two compatible models could act over the same physical region to give the extrapolated value. One example is the scalar diquark model with $F^n/F_2^P \rightarrow_2 0.25$ together with the three-quark correlation plus MMHT2014NNLO with $F_2^n/F_2^P > 0.68$ from Ref. [28], with different weight given to the scalar diquark vs three-quark correlation contribu-tions in order to yield a final ratio of 0.4. Such a scenario would agree with recent results on the nucleon wave func-tion as a linear combination of a three-valence quark state and a quark-diquark state with unequal coefficients in A = 3 nuclei [40,41].

ACKNOWLEDGMENTS

We thank Wally Melnitchouk for helpful discussions and Tyler Kutz for his MARATHON plot. H.V. and F.B. acknowledge support from the National Science Foundation, Award No. Benmokhtar-2012413. J.R.W. is supported by the LDRD programs of LBNL, the EIC Center at Jefferson Lab, and the U.S. Department of Energy, Office of Science, Office of Nuclear Physics, under Contract No. DE-AC02-05CH11231. This research was funded in part by Department of Energy Grant No. DE-AC05-06OR23177 under which the Jefferson Science Associates operates the Thomas Jefferson National Accelerator Facility.

^[1] J. I. Friedman, Deep inelastic scattering: Comparisons with the quark model, Rev. Mod. Phys. **63**, 615 (1991).

^[2] H. W. Kendall, Deep inelastic scattering: Experiments on the proton and the observation of scaling, Rev. Mod. Phys. 63, 597 (1991).

^[3] J. D. Bjorken, Asymptotic sum rules at infinite momentum, Phys. Rev. 179, 1547 (1969).

^[4] D. Abrams et al. (Jefferson Lab Hall A Tritium Collaboration), Measurement of the Nucleon F₂ⁿ/F₂^p Structure Function Ratio by the Jefferson Lab MARATHON Tritium/Helium-3 Deep Inelastic Scattering Experiment, Phys. Rev. Lett. 128, 132003 (2022).

^[5] Jefferson Lab MARATHON Collaboration Proposal, Measurement of the F2n/F2p, d/u RAtios and A=3 EMC Effect

in Deep Inelastic Electron Scattering Off the Tritium and Helium MirrOr Nuclei (2021), https://hallaweb.jlab.org/collab/PAC/PAC37/.

^[6] J. Bane, The EMC effect in A = 3 nuclei, Ph.D. thesis, University of Tennessee, 2019.

^[7] T. Hague, Measurement of the EMC effect of the helium-3 nucleus at Jefferson Lab, Ph.D. thesis, Kent State University, 2020.

^[8] T. T. Kutz, Deep inelastic scattering from A = 3 nuclei: Nucleon structure and the EMC effect, Ph.D. thesis, Stony Brook University, 2019.

^[9] H. Liu, Measurement of the ratio of the neutron to pro-ton structure functions, and the three-nucleon EMC ef-fect in deep inelastic electron scattering off tritium and

- helium-3 mirror nuclei, Ph.D. thesis, Columbia University, 2020
- [10] M. R. Nycz, Measurement of the EMC effect of the tritium nucleus at Jefferson Lab, Ph.D. thesis, Kent State University, 2020.
- [11] T. Su, Measurement of F_2^n/F_2^p from deep inelastic electron scattering off A = 3 mirror nuclei at Jefferson Lab, Ph.D. thesis, Kent State University, 2020.
- [12] M. Breidenbach, J. I. Friedman, H. W. Kendall, E. D. Bloom, D. H. Coward, H. C. DeStaebler, J. Drees, L. W. Mo, and R. E. Taylor, Observed Behavior of Highly Inelastic Electron-Proton Scattering, Phys. Rev. Lett. 23, 935 (1969).
- [13] E. D. Bloom et al., High-Energy Inelastic e-p Scattering at 6° and 10°, Phys. Rev. Lett. 23, 930 (1969).
- [14] W. Melnitchouk and A. W. Thomas, Neutron/proton structure function ratio at large x, Phys. Lett. B 377, 11 (1996).
- [15] R. J. Holt and C. D. Roberts, Distribution functions of the nucleon and pion in the valence region, Rev. Mod. Phys. 82, 2991 (2010).
- [16] S. Dulat, T.-J. Hou, J. Gao, M. Guzzi, J. Huston, P. Nadolsky, J. Pumplin, C. Schmidt, D. Stump, and C. P. Yuan, New parton distribution functions from a global analysis of quantum chromodynamics, Phys. Rev. D 93, 033006 (2016).
- [17] H. L. Lai, J. Huston, S. Kuhlmann, F. I. Olness, J. F. Owens, D. E. Soper, W. K. Tung, and H. Weerts, Improved parton distributions from global analysis of recent deep inelastic scattering and inclusive jet data, Phys. Rev. D 55, 1280 (1997).
- [18] F. E. Close, vW_2 at small ω^0 and resonance form factors in a quark model with broken SU(6), Phys. Lett. B **43**, 422 (1973).
- [19] A. Selem and F. Wilczek, Hadron systematics and emergent diquarks, in *New Trends in HERA Physics 2005* (World Scientific, Singapore, 2006), pp. 337–356.
- [20] N. Isgur, Valence quark spin distribution functions, Phys. Rev. D 59, 034013 (1999).
- [21] T. Liu, R. S. Sufian, G. F. de Téramond, H. G. Dosch, S. J. Brodsky, and A. Deur, Unified Description of Polarized and Unpolarized Quark Distributions in the Proton, Phys. Rev. Lett. 124, 082003 (2020).
- [22] T. Liu, A. Deur, and G. de Teramond (private communication).
- [23] K. D. Bednar, I. C. Cloët, and P. C. Tandy, Nucleon quark distribution functions from the Dyson–Schwinger equations, Phys. Lett. B 782, 675 (2018).
- [24] C. D. Roberts, R. J. Holt, and S. M. Schmidt, Nucleon spin structure at very high-x, Phys. Lett. B 727, 249 (2013).
- [25] H. L. L. Roberts, A. Bashir, L. X. Gutierrez-Guerrero, C. D. Roberts, and D. J. Wilson, π and ρ mesons, and their diquark

- partners, from a contact interaction, Phys. Rev. C 83, 065206 (2011).
- [26] G. R. Farrar and D. R. Jackson, Pion and Nucleon Structure Functions Near *x* = 1, Phys. Rev. Lett. **35**, 1416 (1975).
- [27] S. J. Brodsky, M. Burkardt, and I. Schmidt, Perturbative QCD constraints on the shape of polarized quark and gluon distributions, Nucl. Phys. B 441, 197 (1995).
- [28] C. Leon and M. Sargsian, Residual mean field model of valence quarks in the nucleon, Eur. Phys. J. C 82, 309 (2022).
- [29] J. Kuti and V. F. Weisskopf, Inelastic lepton-nucleon scattering and lepton pair production in the relativistic quark parton model, Phys. Rev. D 4, 3418 (1971).
- [30] Z.-F. Cui, F. Gao, D. Binosi, L. Chang, C. D. Roberts, and S. M. Schmidt, Valence quark ratio in the proton, Chin. Phys. Lett. 39, 041401 (2022).
- [31] C. Cocuzza, C. E. Keppel, H. Liu, W. Melnitchouk, A. Metz, N. Sato, and A. W. Thomas (Jefferson Lab Angular Momentum (JAM) Collaboration), Isovector EMC Effect from Global QCD Analysis with MARATHON Data, Phys. Rev. Lett. 127, 242001 (2021).
- [32] S. A. Kulagin and R. Petti, Global study of nuclear structure functions, Nucl. Phys. A 765, 126 (2006).
- [33] S. A. Kulagin and R. Petti, Structure functions for light nuclei, Phys. Rev. C **82**, 054614 (2010).
- [34] E. P. Segarra, A. Schmidt, T. Kutz, D. W. Higinbotham, E. Piasetzky, M. Strikman, L. B. Weinstein, and O. Hen, Neutron Valence Structure from Nuclear Deep Inelastic Scattering, Phys. Rev. Lett. 124, 092002 (2020).
- [35] A. Accardi, W. Melnitchouk, J. F. Owens, M. E. Christy, C. E. Keppel, L. Zhu, and J. G. Morfin, Uncertainties in determining parton distributions at large x, Phys. Rev. D 84, 014008 (2011).
- [36] A. Accardi, L. T. Brady, W. Melnitchouk, J. F. Owens, and N. Sato, Constraints on large-x parton distributions from new weak boson production and deep-inelastic scattering data, Phys. Rev. D 93, 114017 (2016).
- [37] B. Andersson *et al.* (Small x Collaboration), Small x phenomenology: Summary and status, Eur. Phys. J. C **25**, 77 (2002).
- [38] F. E. Close, An Introduction to Quarks and Partons (Academic Press, San Diego, 1979).
- [39] R. L. Jaffe, Exotica, Phys. Rep. 409, 1 (2005).
- [40] J. Rittenhouse West, Diquark induced short-range nucleonnucleon correlations & the EMC effect, Nucl. Phys. A 1029, 122563 (2023).
- [41] S. Li *et al.*, Revealing the short-range structure of the mirror nuclei ³H and ³He, Nature (London) **609**, 41 (2022).
- [42] B. Efron and R. Tibshirani, *An Introduction to the Bootstrap* (Chapman and Hall/CRC, Boca Raton, FL, 1993).